

Specific heat of an anisotropic superconductor: Nb_3X_4 with $\text{X}=\text{S}, \text{Se}, \text{and Te}$

Hiroiyuki Okamoto, Hiromi Taniguti, and Yutaka Ishihara

Department of Physics, Faculty of Science, Kanazawa University, Kanazawa 920-11, Japan

(Received 1 May 1995; revised manuscript received 8 September 1995)

The specific heats of Nb_3S_4 , Nb_3Se_4 , and Nb_3Te_4 were measured in the temperature range from 0.5 to 30 K. The magnitude of the jump at the superconducting transition temperature T_c was $1.11 \pm 0.02 \gamma T_c$ for Nb_3S_4 and $0.66 \pm 0.01 \gamma T_c$ for Nb_3Se_4 . The superconducting property for both compounds is discussed on the basis of the weak-coupling BCS theory as extended by Clem to include the effects of energy-gap anisotropy. We estimated the mean-squared anisotropy $\langle a^2 \rangle = 0.07 \pm 0.02$ and the reduced-energy gap $2\varepsilon_0/(k_B T) = 3.1 \pm 0.1$ for Nb_3S_4 , and $\langle a^2 \rangle = 0.14 \pm 0.03$ and $2\varepsilon_0/(k_B T) = 2.8 \pm 0.1$ for Nb_3Se_4 . For Nb_3Te_4 , although it becomes superconducting at about 2 K in the electrical-resistivity measurement, an excess of specific heat due to the superconducting transition was not found down to about 0.5 K. We also discuss the superconducting property of Nb_3Te_4 .

I. INTRODUCTION

A number of transition-metal chalcogenides crystallizes in fiber structures¹ which become superconducting at low temperatures^{2,3} or undergo phase transitions due to charge-density-wave (CDW) formation. Owing to the characteristic behavior of CDW's, the properties on charge-density waves have been studied intensively.⁴ However, there has been little reliable information on the thermodynamic properties of those superconductors. This is because only small single crystals are available and their superconducting transition temperatures are much lower than those of usual superconductors. Niobium chalcogenide Nb_3X_4 with $\text{X}=\text{S}, \text{Se}, \text{and Te}$ is one of those kinds of superconductors and has a moderate high transition temperature.⁵ These compounds are, therefore, suitable matters for studying the thermodynamic properties in the superconducting states.

The crystal structures of Nb_3X_4 are isomorphous with each other and belong to a hexagonal crystal system.⁶⁻⁸ The unit cells contain six niobium atoms and eight chalcogens. Each niobium is surrounded by six chalcogens at the corner of a deformed octahedron consisted of NbX_6 . The niobium atoms are shifted from the centers of the octahedra in the direction of faces sharing two edges with other octahedra. Hence zigzag Nb-Nb chains are formed along the c axis. The Nb-Nb distances in the chains (d_{\parallel}) = 2.881, 2.885, and 2.973 Å for $\text{X}=\text{S}, \text{Se}, \text{and Te}$ are comparable to the corresponding value in niobium metal (2.859 Å), while the shortest Nb-Nb distances d_{\perp} between Nb chains are 3.369, 3.567, and 3.854 Å for $\text{X}=\text{S}, \text{Se}, \text{and Te}$. The ratios of d_{\perp}/d_{\parallel} are 1.169, 1.236, and 1.298 in the above order. Hence the anisotropy of the crystal structures increases according to the above order. This large anisotropy leads to weak coupling. Another remarkable feature of the Nb_3X_4 structure is the presence of large infinite void channels along the c axis.

Reflecting the above-mentioned characteristic of the crystal structure, Nb_3X_4 shows high anisotropy in the electrical properties such as resistivity⁹ and critical field.¹⁰⁻¹² Furthermore, the electrical resistivity in both Nb_3S_4 (Ref. 9) and Nb_3Se_4 (Ref. 11) follows a T^3 form below about 80 K which can be explained by the umklapp scattering process in the quasi-one-dimensional band structure.¹³ The thermoelectric

power and resistivity of Nb_3Te_4 show two anomalies at about 20 and 80 K.¹⁴ The anomaly at 80 K is due to a charge-density-wave formation with commensurate-wave vectors.^{15,16} However, a superlattice corresponding to the anomaly at 20 K has not been observed yet. The specific heat of Nb_3S_4 has been measured by Biberacher and Schwenk.¹⁰ In addition, the thermodynamic properties in the superconducting state of Nb_3S_4 have been studied in detail by Okamoto and Ishihara.¹⁷ These properties also show high anisotropies and follow the weak-coupling BCS theory included the effects of an energy-gap anisotropy.

Associated with Nb_3X_4 , owing to the presence of three Nb chains in the unit cell, there exist three conduction bands and corresponding three Fermi surfaces. A calculation of the energy-band structure for Nb_3X_4 has been made in detail by Oshiyama using the linear-combination-of-atomic-orbital method.^{13,18} The calculated Fermi surfaces are reflected the quasi-one-dimensional crystal structures of those crystals: These Fermi surfaces consist of warped planelike sheets. The bandwidths along the chain direction are highly dispersive and are in the range of 1.5–2.5 eV, while those along the interchain directions are quite flat and are of the order of 0.1 eV. The ratios of the conduction-band width along the chain direction to that along the perpendicular direction are 15, 18, and 19 for Nb_3S_4 , Nb_3Se_4 , and Nb_3Te_4 . Bullett¹⁹ and Canadell and Whangbo²⁰ have also obtained similar results for the band structure of Nb_3S_4 using an atomic-orbital method and a tight-binding method.

In this paper we report the specific heats on Nb_3S_4 , Nb_3Se_4 , and Nb_3Te_4 in the temperature range from 0.5 to 30 K. In an earlier work, two of us, on Nb_3S_4 , measured the specific heat in the temperature range from 1.4 to 7 K and obtained the thermodynamic parameters for the superconducting property.¹⁷ The purpose of this work is to measure systematically the specific heat to determine the thermodynamic properties of Nb_3X_4 . Since the previous work on Nb_3S_4 did not apply a magnetic field, the specific-heat measurement was reexamined to improve the accuracy under a magnetic field. We also present a comparison of the experimental results with BCS predictions for both Nb_3S_4 and Nb_3Se_4 . As a result, we clarify the anisotropy and weak-

coupling effects. Further, we discuss the superconducting property of Nb_3Te_4 .

II. EXPERIMENTAL PROCEDURE

Single crystals of Nb_3X_4 were prepared by an iodine vapor transport method following Nakada and Ishihara^{21,22} on the basis of the earlier work of Ruysink *et al.*⁷ Grown crystals were always fibers. The crystals were examined by Weissenberg-photography analysis and were identified to be Nb_3S_4 , Nb_3Se_4 , and Nb_3Te_4 . Needlelike crystals were elongated parallel to the c axis, which were confirmed by an x-ray oscillation photography method.

The specific heat of Nb_3X_4 was measured using a thermal-relaxation method²³ in the temperature range from 1.4 to 30 K for Nb_3S_4 and from 0.5 to 30 K for both Nb_3Se_4 and Nb_3Te_4 . The measurement was carried out in both zero magnetic field and a magnetic field of 14 kOe. The magnetic field was applied perpendicular to the c axis. For this direction to the crystal axis of the applied field, Nb_3X_4 has the lowest value of the upper critical field H_{c2} : about 5 kOe at 0 K for Nb_3S_4 .¹⁰ Several single crystals of total mass of about 50 mg were greased to a sapphire bolometer with the addenda contributing about 10% to the heat capacity. The temperature of a sample was measured using a carbon-resistance thermometer below 7 K and a silicon diode thermometer above 7 K placed in close proximity to the sample. The carbon thermometer was calibrated in each run by comparing the resistor with a germanium thermometer.

As a test of the measurement apparatus, we measured the specific heat of an indium sample weighing 47 mg at temperatures between 1.5 and 9 K. The purity of the indium sample was 99.999%. The result was compared to the results of O'Neal and Phillips,²⁴ who measured an indium sample by the adiabatic-calorimeter method. Our result agreed to within 0.5% with theirs. The error in the specific heat of Nb_3X_4 was about 4% below 1.4 K and 1% above 1.4 K, mainly due to the small mass of the sample used in the experiment.

III. RESULTS

Figure 1 shows the temperature dependence of the specific heat C of Nb_3S_4 plotted as C/T vs T^2 , where open and solid circles are data in zero magnetic field and in a field of 14 kOe. In Fig. 1, the data for this compound have been plotted on an expanded scale for the temperature range below 5.5 K. The jump ΔC at $T_c=3.78$ K in the specific heat for zero field is due to the superconducting transition. The midpoint of the jump is defined as the superconducting-transition temperature T_c . This value is slightly small compared to that ($T_c=4.0$ K in Ref. 5) determined by the measurement of the electrical resistivity. The width of the transition temperature is 0.14 K. The specific heat in the normal state is given by

$$C = \gamma T + \beta T^3 \quad (1)$$

in the temperature range from 1.4 to 13 K. The solid line in Fig. 1 represents the least-squares fit of this equation to the data under the magnetic field with $\gamma=13.6\pm0.1$ mJ/(mol K²) and $\beta=0.328\pm0.004$ mJ/(mol K⁴). The magnitude of the

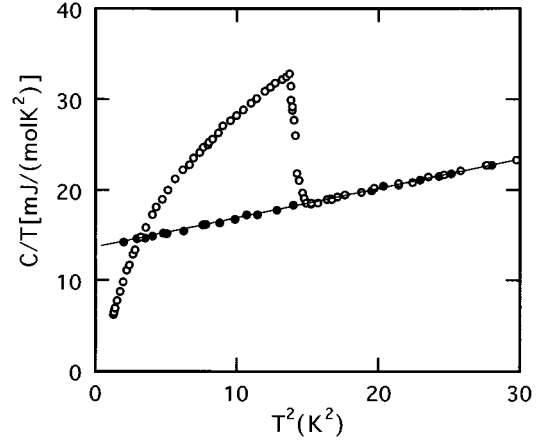


FIG. 1. Specific heat of Nb_3S_4 plotted as C/T vs T^2 . Open and solid circles are data for zero magnetic field and a magnetic field of 14 kOe. Solid line shows the least-squares fit to data under a magnetic field from 1.4 to 12 K given by $C/T = \gamma + \beta T^2$ with $\gamma=13.6 \pm 0.1$ mJ/(mol K²) and $\beta=0.328 \pm 0.004$ mJ/(mol K⁴).

normalized jump $\Delta C/(\gamma T_c)$ is 1.11 ± 0.02 . The Debye temperature is given by $\Theta_D = (12/5)(\pi^4 n R / \beta)$, where R is the gas constant and n is the number of atoms per molecule ($n=7$ for Nb_3X_4). Using our experimental value of β , this expression gives $\Theta_D = 346 \pm 2$ K.

In order to evaluate the electron-phonon coupling constant λ , we use McMillan's expression²⁵

$$T_c = \frac{\Theta_D}{1.45} \exp \left[- \frac{1.04(1 + \lambda)}{\lambda - \mu^*(1 + 0.62\lambda)} \right], \quad (2)$$

where μ^* denotes the Coulomb repulsion between electrons. Here we assume empirically $\mu^*=0.1$. Using Eq. (2) with $T_c=3.78$ K and $\Theta_D=346$ K, we obtain $\lambda=0.51$. We further estimated the electronic density of states $D(\epsilon_F)=1.9$ states/eV molecule at the Fermi level using the formula $\gamma = (2/3)\pi^2 k_B^2 (1 + \lambda) D(\epsilon_F)$, where k_B is Boltzmann's constant. The results of the specific-heat measurement and the analysis for Nb_3S_4 are shown in Tables I and II. These values are in good agreement with the previous result¹⁷ except for the γ value. The present value of $\gamma=13.6$ mJ/(mol K²) is 14% larger than the previous result (11.7 mJ/mol K²), but

TABLE I. Fundamental parameters obtained from the specific-heat measurements.

	Nb_3S_4	Nb_3Se_4	Nb_3Te_4
T_c (K)	3.78	2.31	1.95 ^a
γ [mJ/(mol K ²)]	13.6 ± 0.1	21.4 ± 0.2	18.7 ± 0.8
β [mJ/(mol K ⁴)]	0.328 ± 0.004	1.27 ± 0.02	11.4 ± 0.03
Θ_D (K)	346 ± 2	220 ± 2	106 ± 1
λ^b	0.51	0.51	0.59
$D(\epsilon_F)^b$ [states/(eV molecule)]	1.9	3.0	2.5

^aValue determined from the resistive-transition curve.

^bValues of $\lambda=0.414$ and $D(\epsilon_F)=1.76$ in Table I of Ref. 17 are errors of 0.51 and 1.9. If we assume $\mu^*=0.13$, for example, in Nb_3S_4 , these values become $\lambda=0.57$ and $D(\epsilon_F)=1.8$.

TABLE II. Thermodynamic parameters in the superconducting states. Values of the BCS prediction are shown for comparison.

	Nb ₃ S ₄	Nb ₃ Se ₄	BCS
$\Delta C/(\gamma T_c)$	1.11 ± 0.02	0.66 ± 0.01	1.43
$\langle a^2 \rangle$	0.07 ± 0.02	0.14 ± 0.03	0
$2\varepsilon_0/(k_B T_c)$	3.1 ± 0.1	2.8 ± 0.1	3.52
$2\pi\gamma[T_c/H_c(0)]^2$	1.21 ± 0.04	1.36 ± 0.07	1.06
$H_c(0)$ (Oe)	353 ± 4	244 ± 3	

15% smaller than that of Biberacher and Schwenk (15.6 mJ/mol K²). The magnitude of γ is somewhat different from sample to sample and appears to be sensitive to the quality of the sample used.

Figure 2 shows the temperature dependence of the specific heat of Nb₃Se₄ plotted as C/T vs T^2 , where open and solid circles are data in zero magnetic field and in a field of 14 kOe. In Fig. 2, the data for Nb₃Se₄ have been plotted on an expanded scale for the temperature range below 3.2 K. The jump at $T_c=2.31$ K in the specific heat for zero field is also due to the superconducting transition. The transition temperature was determined in the same way as Nb₃S₄. However, the value is somewhat larger than that ($T_c=2.0$ K in Ref. 5) determined by the measurement of the electrical resistivity. The width of the transition temperature is about 0.2 K. The specific heat in the normal state is given by Eq. (1) in the temperature range from 1.4 to 7 K. The solid line in Fig. 2 is the least-squares fit of Eq. (1) to the data under a magnetic field with $\gamma=21.4 \pm 0.2$ mJ/(mol K²) and $\beta=1.27 \pm 0.02$ mJ/(mol K⁴). The magnitude of $\Delta C/(\gamma T_c)$ is 0.66 ± 0.01 . The results of our measurement for Nb₃Se₄ are shown in Tables I and II. From these results we estimated the values of Θ_D , λ , and $D(\varepsilon_F)$ in the same way as Nb₃S₄, as shown in Table I.

Figure 3 shows the temperature dependence of the specific heat of Nb₃Te₄ plotted as C/T vs T^2 , where open circles are data in zero magnetic field and solid circles above 1.4 K

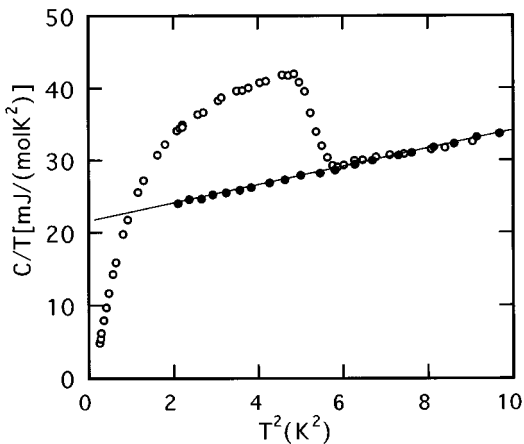


FIG. 2. Specific heat of Nb₃Se₄ plotted as C/T vs T^2 . Open and solid circles are data for zero magnetic field and a magnetic field of 14 kOe. Solid line shows the least-squares fit to data under a magnetic field from 1.4 to 6 K given by $C/T = \gamma + \beta T^2$ with $\gamma=21.4 \pm 0.2$ mJ/(mol K²) and $\beta=1.27 \pm 0.02$ mJ/(mol K⁴).

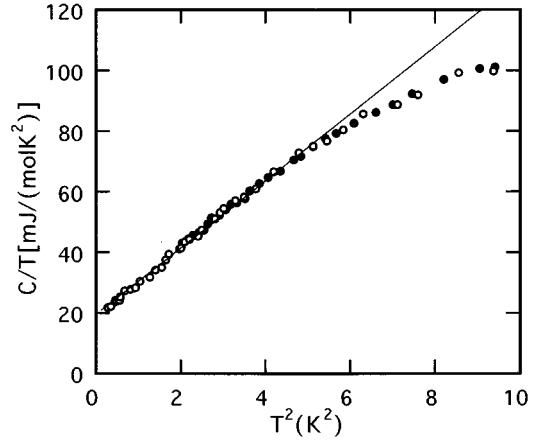


FIG. 3. Specific heat of Nb₃Te₄ plotted as C/T vs T^2 . Open and solid circles are data for zero magnetic field and a magnetic field of 14 kOe. Solid line shows the least-squares fit to data 0.5 to 2.1 K given by $C/T = \gamma + \beta T^2$ with $\gamma=18.7 \pm 0.8$ mJ/(mol K²) and $\beta=11.4 \pm 0.3$ mJ/(mol K⁴).

are data in a field of 14 kOe. In Fig. 3, the data for Nb₃Te₄ have been plotted on an expanded scale for the temperature range below 3.2 K. The results for both zero field and applied field are in agreement with each other. Although the superconductivity of Nb₃Te₄ has been observed at about 2 K by the measurement of the electrical resistivity,^{5,12} no anomaly was found in the specific heat down to 0.5 K within the experimental accuracy. The specific heat in the temperature range from 0.5 to 2.1 K can be approximated by Eq. (1). We will later discuss this approximation. The solid line in Fig. 3 is the least-squares fit of Eq. (1) to these data with $\gamma=18.7 \pm 0.8$ mJ/(mol K²) and $\beta=11.4 \pm 0.3$ mJ/(mol K⁴). The values of Θ_D , λ , and $D(\varepsilon_F)$ were also obtained in the same way as Nb₃S₄. These values are shown in Table I. However, for the estimation of λ , we used $T_c=1.95$ K determined from the resistive-transition curve.

The thermodynamic critical field $H_c(T)$ for Nb₃S₄ and Nb₃Se₄ was obtained as a function of temperature using the specific-heat data in both the normal and superconducting states. The difference in entropy $\Delta S(T)$ between the normal and superconducting states was obtained through the thermodynamic relation

$$\Delta S(T) = S_n(T) - S_s(T) = \gamma T + (1/3)\beta T^3 - \int_0^T (C_s/T') dT',$$

where $S_n(T)$ and $S_s(T)$ are the entropies in the normal and superconducting states, and C_s is the specific heat in the superconducting state. Hence $H_c(T)$ was obtained by numerical integration of the $\Delta S(T)$ curve, from

$$H_c(T)^2 = \frac{8\pi}{V} \int_T^{T_c} \Delta S(T') dT', \quad (3)$$

where V is the molar volume of Nb₃X₄. Figure 4 shows $H_c(T)$ for Nb₃S₄ (solid circles) and Nb₃Se₄ (open circles). The calculated values of $H_c(0)$ are 353 ± 4 Oe for Nb₃S₄ and 244 ± 3 Oe for Nb₃Se₄. The present value of $H_c(0)$ for Nb₃S₄ is 15 Oe, large compared with that of the previous result.¹⁷ This disagreement with the previous value is due to the im-

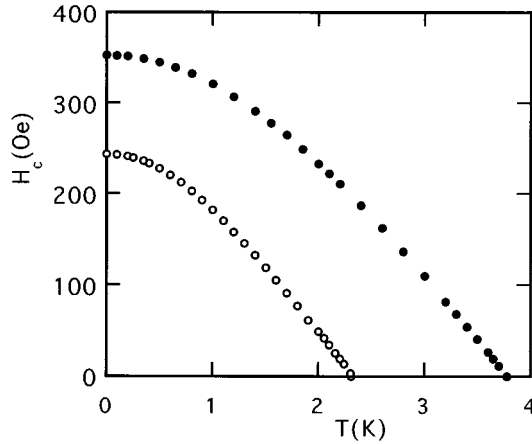


FIG. 4. Temperature dependence of $H_c(T)$. Solid and open circles are data for Nb_3S_4 and Nb_3Se_4 .

provement of the accuracy, because the temperature range that Eq. (1) holds true expands from T_c to lower temperature. Figure 5 shows the deviation $D(t)$ of $h = H_c(t)/H_c(0)$ from the parabolic law plotted as $D(t)$ vs t^2 , where $D(t) = h - (1 - t^2)$ and $t = T/T_c$. In this figure, solid and open circles are $D(t)$ for Nb_3S_4 and Nb_3Se_4 ; here, the BCS prediction is shown by open squares for comparison. The absolute values of $D(t)$ increase in the following order: BCS prediction, Nb_3S_4 , Nb_3Se_4 . The values of $H_c(0)$ for Nb_3S_4 and Nb_3Se_4 are shown in Table II.

IV. DISCUSSION

The specific-heat jump of Nb_3S_4 ($1.11\gamma T_c$) is substantially small as compared with the BCS value of $1.43\gamma T_c$,²⁶ while that of Nb_3Se_4 ($0.66\gamma T_c$) is less than half of the BCS value. The values of λ for Nb_3X_4 are close to the weak-coupling limit compared to $\lambda \approx 0.8$ of Nb (Ref. 25) and NbSe_2 ,²⁷ which are considered to be intermediate strong-coupling superconductors. The curves of $D(t)$ for both

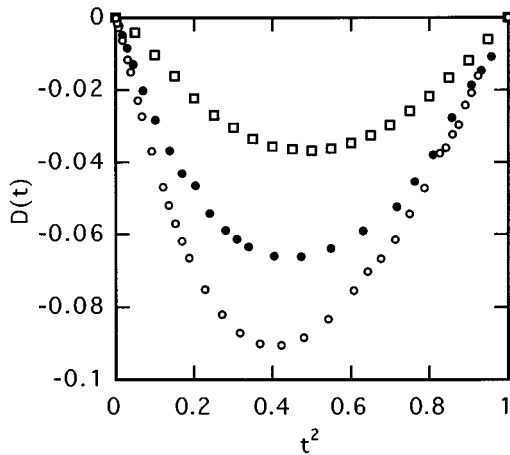


FIG. 5. Deviation function $D(t) = h - (1 - t^2)$ for Nb_3S_4 and Nb_3Se_4 , where $t = H_c(t)/H_c(0)$ and $t = T/T_c$. Solid and open circles are data for Nb_3S_4 and Nb_3Se_4 . The BCS prediction is also shown by open squares for comparison.

Nb_3S_4 and Nb_3Se_4 lie below that of the BCS isotropic-gap model. Such behavior can, therefore, be treated within the weak-coupling BCS theory. In weak-coupling superconductors, these phenomena are interpreted in terms of the presence of an energy-gap anisotropy: When the energy gap is anisotropic, there is a thermal selection of participating quasiparticles. At lower temperature, electrons related to the smaller energy gap can be contributed to the electronic specific heat. Clem has calculated the effects of an anisotropic-energy gap on the thermodynamic properties of superconductors.²⁸ His results lead to the following modifications in the thermodynamic properties of the BCS prediction:

$$2\varepsilon_0/(k_B T_c) = 3.528(1 - 3\langle a^2 \rangle/2), \quad (4)$$

$$2\pi\gamma[T_c/H_c(0)]^2 = 1.057(1 + 2\langle a^2 \rangle), \quad (5)$$

$$\Delta C/(\gamma T_c) = 1.426(1 - 4\langle a^2 \rangle), \quad (6)$$

where ε_0 is the averaged energy gap at 0 K and $\langle a^2 \rangle$, the mean-squared anisotropy, is the average over the Fermi surface of the square of the deviation of the energy-gap parameter from its average. The values of $\langle a^2 \rangle$ calculated from Eqs. (5) and (6) are 0.07 and 0.06 for Nb_3S_4 and are 0.15 and 0.13 for Nb_3Se_4 . Both compounds have much larger mean-squared anisotropies than that of the layer compound 2H-NbSe_2 ($\langle a^2 \rangle \approx 0.04$).²⁷ The value of $\langle a^2 \rangle$ increases in the order of increasing lattice anisotropy in these compounds. Hence these large values may be due to the filamentary nature of these compounds. Using the average value of $\langle a^2 \rangle = 0.07 \pm 0.02$ for Nb_3S_4 and $\langle a^2 \rangle = 0.14 \pm 0.03$ for Nb_3Se_4 , the values of $2\varepsilon_0/(k_B T_c)$ are obtained to be 3.1 ± 0.1 for Nb_3S_4 and 2.8 ± 0.1 for Nb_3Se_4 . These values are listed in Table II.

As mentioned above, Nb_3Te_4 becomes superconducting at about 2 K in the electrical-resistivity measurement. Nevertheless, the specific heat in Nb_3Te_4 changed smoothly and continuously with temperature down to about 0.5 K and did not show a characteristic of superconducting transition near T_c . Further, in order to investigate the thermodynamic state of Nb_3Te_4 , the magnetization of Nb_3Te_4 was measured by an ac mutual inductance method down to about 0.5 K. No trace of a Meissner effect was observed down to 1.4 K, and the effect occurred appreciably below about 1.4 K. The susceptibility nearly saturated at 0.6 K and reached about 90% of $-1/4\pi$ at about 0.5 K. At a glance, this result suggests that the superconductivity of Nb_3Te_4 is at least a bulk effect below 1.4 K. However, such a result is in conflict with the result of the specific-heat measurement. One possible explanation for this discrepancy is as follows.

The crystal structure of Nb_3Te_4 consists of Nb chains running along the c axis, as described in Sec. I. The distance between the Nb atoms in a chain is metallic, but the inter-chain distance exceeds the metallic distance. Hence Nb_3Te_4 is regarded as an aggregate of one-dimensional chains that are weakly coupled through Josephson-type junctions. In such a superconductor, ac susceptibility measurements can lead to quite erroneous results due to filamentary superconductivity. Very small superconducting volume fractions may shield the entire sample if the superconducting regions are physically connected by such as Josephson junctions. On the contrary, specific-heat measurements detect only true bulk

superconductivity. For this reason, the result of the specific-heat measurement at low temperatures indicates that the superconductivity of Nb_3Te_4 is filamentary. We intend to study in more detail the susceptibility of Nb_3Te_4 in order to test this hypothesis.

Now we consider the thermodynamic state of Nb_3Te_4 at low temperatures. Since the Meissner effect was not observed down to 1.4 K and the magnitude of the upper critical field¹² is substantially smaller than the applied field, the specific heat above 1.4 K under a magnetic field is that of the normal state. Furthermore, the specific heat below 1.4 K can be regarded as that of the normal state with a good approximation. This is because the specific heat below 1.4 K can be expressed by extrapolation of the straight line approximation for the normal state in Fig. 3.

In summary, we measured the specific heats of Nb_3S_4 , Nb_3Se_4 , and Nb_3Te_4 in the normal and superconducting states. The magnitude of the specific-heat jump decreased in

the order Nb_3S_4 , Nb_3Se_4 . The behavior of the specific heat in the superconducting state for both Nb_3S_4 and Nb_3Se_4 may be accounted for by the weak-coupling BCS theory included an anisotropic-energy gap. The mean-squared anisotropies $\langle a^2 \rangle$ are 0.07 ± 0.02 and 0.14 ± 0.03 for Nb_3S_4 and Nb_3Se_4 . The normalized energy gaps $2\epsilon_0/(k_B T_c)$ are 3.1 ± 0.1 and 2.8 ± 0.1 for Nb_3S_4 and Nb_3Se_4 . Such thermodynamic behavior indicates that both compounds are highly anisotropic and weak-coupling superconductors. Detailed confirmation of this interpretation will require studies of the energy gap of Nb_3S_4 and Nb_3Se_4 through the measurements of the specific heat with a high accuracy down to more low temperature, tunneling spectroscopy measurements, or other techniques which yield less of a macroscopic average than the specific heat. In Nb_3Te_4 , no trace of the superconducting transition was found in the specific heat down to about 0.5 K. This result indicates that Nb_3Te_4 is a filamentary superconductor.

¹ See, for example, *Extended Linear Chain Compounds*, edited by J. S. Miller (Plenum, New York, 1982).

² R. L. Greene, G. B. Street, and L. J. Suter, *Phys. Rev. Lett.* **34**, 577 (1975).

³ W. W. Fuller, P. N. Chaikin, and N. P. Ong, *Phys. Rev. B* **24**, 1333 (1981).

⁴ See, for example, *Electronic Properties of Inorganic Quasi 1D Compounds*, edited by P. Monceau (Reidel, Dordrecht, 1985).

⁵ E. Amberger, K. Polborn, M. Dietrich, B. Obst, and P. Grimm, *Solid State Commun.* **26**, 943 (1978).

⁶ K. Selte and A. Kjekshus, *Acta Crystallogr.* **17**, 1568 (1964).

⁷ A. F. J. Ruysink, F. Kadijk, A. J. Wagner, and F. Jellinek, *Acta Crystallogr. B* **24**, 1614 (1968).

⁸ J. G. Smeggil, *J. Solid State Chem.* **3**, 248 (1971).

⁹ Y. Ishihara and I. Nakada, *Solid State Commun.* **42**, 579 (1982).

¹⁰ W. Biberacher and H. Schwenk, *Solid State Commun.* **33**, 385 (1980).

¹¹ Y. Ishihara and I. Nakada, *Solid State Commun.* **44**, 1439 (1982).

¹² Y. Ishihara and I. Nakada, *Solid State Commun.* **45**, 129 (1983).

¹³ A. Oshiyama, *J. Phys. Soc. Jpn.* **52**, 587 (1983).

¹⁴ Y. Ishihara, I. Nakada, K. Suzuki, and M. Ichihara, *Solid State Commun.* **50**, 657 (1984).

¹⁵ K. Suzuki, M. Ichihara, I. Nakada, and Y. Ishihara, *Solid State Commun.* **52**, 743 (1984).

¹⁶ T. Sekine, Y. Kiuchi, E. Matsuura, K. Uchinokura, and R. Yoshizaki, *Phys. Rev. B* **36**, 3153 (1987).

¹⁷ H. Okamoto and Y. Ishihara, *Phys. Rev. B* **48**, 3927 (1993).

¹⁸ A. Oshiyama, *Solid State Commun.* **43**, 607 (1982).

¹⁹ D. W. Bullett, *J. Solid State Chem.* **33**, 13 (1980).

²⁰ E. Canadell and M.-H. Whangbo, *Inorg. Chem.* **25**, 1488 (1986).

²¹ I. Nakada and Y. Ishihara, *Jpn. J. Appl. Phys.* **23**, 677 (1984).

²² I. Nakada and Y. Ishihara, *Jpn. J. Appl. Phys.* **24**, 31 (1985).

²³ R. Bachmann, F. J. DiSalvo, T. H. Geballe, R. L. Greene, R. E. Howard, C. N. King, H. C. Kirsch, K. N. Lee, R. E. Schwall, H.-U. Thomas, and R. B. Zubeck, *Rev. Sci. Instrum.* **43**, 205 (1972).

²⁴ H. R. O'Neal and N. E. Phillips, *Phys. Rev.* **137**, A748 (1965).

²⁵ W. L. McMillan, *Phys. Rev.* **167**, 331 (1968).

²⁶ J. Bardeen, L. N. Cooper, and J. R. Schrieffer, *Phys. Rev.* **108**, 1175 (1957).

²⁷ N. Kobayashi, K. Noto, and Y. Muto, *J. Low Temp. Phys.* **27**, 217 (1977).

²⁸ J. R. Clem, *Ann. Phys. (N.Y.)* **40**, 268 (1966).